

2023

Calibration of Perfluorinated Alkyl Acid Uptake Rates by a Tube Passive Sampler in Water

Matthew Dunn
University of Rhode Island

Jitka Becanova
University of Rhode Island, becanova@uri.edu

Jarod Snook
University of Rhode Island

Bridger Ruyle

Rainer Lohmann
Follow this and additional works at: <https://digitalcommons.uri.edu/gsofacpubs>
University of Rhode Island, rlohmann@uri.edu

The University of Rhode Island Faculty have made this article openly available.
Please let us know how Open Access to this research benefits you.

This is a pre-publication author manuscript of the final, published article.

Terms of Use

This article is made available under the terms and conditions applicable towards Open Access Policy Articles, as set forth in our [Terms of Use](#).

Citation/Publisher Attribution

Dunn, M., Becanova, J., Snook, J., Ruyle, B. & Lohmann, R. (2023). Calibration of Perfluorinated Alkyl Acid Uptake Rates by a Tube Passive Sampler in Water. *ACS EST Water*, 3(2), 323-341. <https://doi.org/10.1021/acsestwater.2c00384>

Available at: <https://doi.org/10.1021/acsestwater.2c00384>

This Article is brought to you for free and open access by the Graduate School of Oceanography at DigitalCommons@URI. It has been accepted for inclusion in Graduate School of Oceanography Faculty Publications by an authorized administrator of DigitalCommons@URI. For more information, please contact digitalcommons@etal.uri.edu.

1 **Calibration of Perfluorinated Alkyl Acid Uptake Rates by a Tube Passive Sampler in**
2 **Water**

3

4 **Matt Dunn¹, Jitka Becanova¹, Jarod Snook¹, Bridger Ruyle², Rainer Lohmann^{1,*}**

5 ¹ Graduate School of Oceanography, University of Rhode Island, 215 South Ferry Rd, Narragansett,
6 02882 RI, USA

7 ² Harvard John A. Paulson School of Engineering and Applied Science, Harvard University,
8 Cambridge, MA, USA,

9

10 * Corresponding author: Email: rlohmann@uri.edu; Tel (401)874-6612

11

12 **Abstract**

13 Per- and polyfluoroalkyl substances (PFAS) are a group of 4000+ man-made compounds of great
14 concern due to their environmental ubiquity and adverse effects. Despite a general interest, few
15 reliable detection tools for integrative passive sampling of PFAS in water are available. A

16 microporous polyethylene tube with a hydrophilic-lipophilic balance sorbent could serve as a flow-
17 resistant passive sampler for PFAS. The tube's sampling rate, R_s , was predicted based on either
18 partitioning and diffusion, or solely diffusion. At 15 °C, the laboratory measured R_s for

19 perfluorohexanoic acid of $100 \pm 81 \text{ mL day}^{-1}$ were better predicted by a partitioning and diffusion
20 model ($48 \pm 1.8 \text{ mL day}^{-1}$) across $10\text{-}60 \text{ cm s}^{-1}$ water flow speeds ($15 \pm 4.2 \text{ mL day}^{-1}$ diffusion only).

21 For perfluorohexane sulfonate, R_s at 15 °C were similarly different ($110 \pm 60 \text{ mL day}^{-1}$ measured,
22 120 ± 63 versus $12 \pm 3.4 \text{ mL day}^{-1}$ in respective models). R_s values from field deployments were in-
23 between these estimates ($46 \pm 40 \text{ mL day}^{-1}$ for perfluorohexanoic acid). PFAS uptake was not
24 different for previously biofouled membranes in the laboratory, suggesting the general applicability of
25 the sampler in environmental conditions. This research demonstrates that the polyethylene tube's

26 sampling rates are sensitive to the parameterization of the models used here and partitioning-
27 derived values should be used.

28

29 **Key Words:**

30 PFAS, Passive Sampling, Sampling Rate, Numerical Model, Environmental Monitoring, PFHxA,
31 PFHxS

32

33 **Synopsis:**

34 A tube passive sampler design was investigated for deriving sampling rates of nine PFAA with good
35 agreement between measurements in the laboratory, field, and model derived values.

36

37 **1. Introduction**

38 Per- and polyfluorinated alkyl substances (PFAS) are a group man-made compounds that
39 have been identified as contaminants of emerging concern. For decades, PFAS have been used in
40 the production of fluoropolymers, water and stain proof surfaces, non-stick cookware, food contact
41 materials, and aqueous film forming foams (AFFF) used to fight hydrocarbon fires.^{1,2,3,4} Several
42 PFAS pose a wide range of adverse human health impacts due to their ability to bioaccumulate,
43 persist, and be passed on from mother to infant.^{5,6} PFAS have been ubiquitously detected in
44 environmental matrices including drinking water, biota, sediments, air, and human serum.^{7,8,9,10,11,12}
45 Specific human health effects include negative impacts on immune system response, obesity and
46 high cholesterol risks, and increased tumor incidence associated with specific cancers.⁵ Some
47 PFAS, most notably perfluorooctanoic acid (PFOA) and perfluorooctane sulfonic acid (PFOS) have
48 been phased out from production in the US and in the European Union.^{4,13} However, the United
49 States' current regulations are narrowly focused on PFOA and PFOS despite the potential
50 occurrence of over 4000 PFAS compounds of variable chemistry, in contrast to the European
51 Union's attempt to eliminate the use of additional PFAS.^{13,14,15}

52 Concerns over the presence and effects of PFAS have increased the need for affordable and
53 reliable tools for monitoring and investigating environmental PFAS contamination. Passive sampling
54 is a low-cost alternative to traditional (active) water grab sampling that requires no power source for
55 in-situ deployments.^{16,17} The unique chemistry of PFAS makes most traditional equilibrium-based
56 passive sampling technology not applicable for monitoring ionic PFAA in water. Instead, existing
57 passive samplers for PFAS are typically operating in linear uptake as integrative samplers, such as
58 the polar organic chemical integrative sampler (POCIS) design.^{18,19,20,21,22} To reduce the impact of
59 flow on uptake reported in studies using POCIS, we tested a passive sampler with a thicker
60 membrane first introduced for passive sampling of glyphosate, aminomethyl phosphonic acid
61 (AMPA), and PFAS in groundwater.^{19,23,24,25,26,27} This tube passive sampler possesses a 0.2 cm thick
62 microporous high density polyethylene (HDPE) membrane in contrast to the 0.014 cm thick
63 membranes reported for POCIS deployments.^{23,24}

64 Integrative samplers report time weighted averages of water concentrations that can give a
65 more representative depiction of surface water contamination across diurnal, tidal, and seasonal
66 trends than discrete grab sampling.^{18,24,27,28,29,30,31} Other passive sampler designs such as the
67 diffusive gradient in thin film (DGT) samplers have been investigated for PFAS in surface
68 waters.^{32,33,34,35} Recently, an equilibrium-based sampler for PFAS was investigated, using modified
69 nanographene hydrogel to create a water-based sampler as opposed to sorbent-based sampler.³⁶
70 This study was hence performed to calibrate and validate an integrative passive sampler based on a
71 microporous polyethylene tube sampler filled with sorbent for the accumulated of dissolved PFAS in
72 surface waters.

73 Integrative passive samplers require a thorough understanding of sampling rates (R_s , volume
74 per time) that relate the accumulated mass of the target compounds to environmental
75 concentrations. The transfer of analyte from water into the sampler can be described (see Equation
76 1) using the overall mass transfer (k_0) of a dissolved polar organic compound separated into three

77 main steps: mass transfer through the water boundary layer (k_w), transfer through the membrane
78 (k_m), and finally through the sorbent (k_s) with units of velocity for all three transfers:

79
$$\frac{1}{k_0} = \frac{1}{k_w} + \frac{1}{k_m K_{mw}} + \frac{1}{k_s K_{sw}} \text{ (eqn 1),}$$

80 where K_{mw} is the partitioning constant (g water per g HDPE) for a given compound between the
81 membrane and water, and

82 K_{sw} is the partitioning between the sorbent and water (g water per g sorbent).^{17,20, 32, 34,35}

83

84 This model can be adjusted to reflect the unique chemistry of each PFAS, and the properties
85 of the microporous membrane and sorbent used in the tube passive sampler for PFAS. The use of a
86 thick membrane suggests that resistance through this barrier will dominate uptake kinetics.³⁷ The
87 transport through the water boundary layer (k_w) can be estimated using a numerical approach
88 recently published.³⁸ This numerical method was used to estimate k_m and k_s based on the thickness
89 of each barrier and the diffusion through each barrier²⁷. The latter diffusion was calculated as the
90 aqueous diffusivity multiplied by the porosity of the barrier. We assume that all diffusion transport is
91 through the pore spaces of the membrane and sorbent, with only adsorption processes as opposed
92 to absorption.

93 While we assume that mass transfer is rate-limited by diffusion across the membrane, not the
94 sorbent layer, both terms are retained in the equation to verify this.³⁷ Equation 1 is then rearranged,
95 with the k_s and k_m terms substituted as follows (eqn 2):

96
$$\frac{1}{k_0} = \frac{1}{k_w} + \frac{d_m}{K_{mw} * (D_w * \phi_m)} + \frac{d_{sbl}}{K_{sw} * (D_w * \phi_s)} \text{ (eqn 2)}$$

97

98 where D_w is the aqueous diffusion of a PFAS compound ($\text{cm}^2 \text{ s}^{-1}$),

99 ϕ is the porosity of the membrane (ϕ_m) and sorbent (ϕ_s , in %), and

100 d (cm) are the thicknesses of the membrane (d_m) and sorbent boundary layer (d_{sbl}).²⁷

101

102 With this model, the sampling rate can be predicted, and investigated across many
103 environmental parameters including water flow speed, water temperature, water viscosity, as well as
104 physical parameters associated with sampler designs including membrane types and different
105 sorbent choices using equation 3 where A (cm^2) is the total surface area of the tube passive
106 sampler:

$$107 \quad \frac{1}{R_s} = \frac{1}{k_0 * A} \text{ (eqn 3)}$$

108 Sampling rate ($\text{cm}^3 \text{ second}^{-1}$) can then be used as the conversion between mass of a given
109 PFAS compound accumulated within the sampler to the time weighted average concentration in the
110 water during the deployment length (eqn 4):.

$$111 \quad C_w = \frac{N_s}{(R_s * 86.4) * t} \text{ (eqn 4),}$$

112 Where C_w is the time weighted average water concentration (ng L^{-1}),

113 R_s is converted to L day^{-1} , by the conversion factor of 86.4

114 N_s is the mass of a PFAS compound measured in the sampler (ng), and

115 t is the length of the deployment (days).

116

117 Equation 4 can also be rearranged to calculate a sampling rate for experimentally deployed
118 passive samplers with known water concentrations in a laboratory setting. The use of this simple
119 adjusted model can be compared to a more recent derivation of the model that has been highlighted
120 for use with disk-shaped samplers in the literature which provides a more detailed model for steady
121 state conditions in the sorbent layer.³⁷

$$122 \quad \frac{1}{k_0} = \frac{1}{k_w} + \frac{d_m * \tau_m^2}{(D_w * \phi_m)} + \frac{d_{sbl} * \tau_s^2}{(D_w * \phi_s)} \text{ (eqn 5),}$$

123

124 where d_{sbl} is the assumed thickness of the sorbent boundary layer at steady state conditions, which

125 is $0.33 * \text{the half thickness of the sorbent}$,

126 τ_m is the tortuosity of the flow path through the membrane pore space, which is always
127 assumed to be 1, and
128 τ_s is the tortuosity of the flow path through the sorbent bed, which is assumed to be 1.3 from
129 other sorbent modeling literature.²⁶
130

131 Most prior work reported calculated sampling rates for PFAS by POCIS sampler.^{25,33,31} The
132 use of a thick, polyethylene membrane could then be a favorable alternative to previously tested
133 passive samplers, with a lower partitioning PFAS to the membrane, an increased duration of the
134 linear uptake phase and a reduced flow dependency.²⁶

135 In summary, the purpose of this study was to (i) validate the uptake of PFAS in the tube
136 passive sampler in a tank under controlled laboratory conditions (ii) investigate the impacts of flow,
137 temperature, and biofouling on the measured and modeled sampling rates of selected PFAS, and
138 (iii) assess the performance of PFAS mass transfer modeling approaches from the literature for
139 integrative passive samplers.
140

141 **Materials & Methods**

142 **Chemicals and Reagents.** Liquid chromatography-grade methanol (LC-MeOH), and water
143 (LC-water) were purchased from Fisher Scientific (New Hampshire, USA) along with ammonium
144 hydroxide (NH₄OH), ammonium acetate (C₂H₇NO₂), ACS-grade ethanol (EtOH) and ACS-grade
145 methanol (MeOH). Analytical standards were used to create native compound standards from the
146 Wellington PFAC-30PAR mix plus an additional four analytical compounds (Table S1). Mass labeled
147 surrogate solutions were derived from Wellington Laboratories' MPFAC-30ES plus an additional
148 three mass labeled compounds purchased from Wellington Laboratories (Canada). Standards with a
149 range of purity (94-98%) were used to create spiking solutions for all laboratory experiments and
150 consisted of 24 individual compounds purchased from Toronto Research Chemicals (Canada),
151 SynQuest (Florida, USA), Apollo Scientific (United Kingdom), and Santa Cruz (Texas, USA) (S1).

152 Solutions were created from solid standards and diluted in LC-MeOH before being stored in the
153 refrigerator while awaiting use. Only 9 PFAA compounds (the C4-C8 PFCA and the C4-C8 PFSA)
154 have published aqueous diffusivities, an important parameter for the modeling of sampler uptake.
155 These 9 PFAA were included in the twenty-four-mix spiked into the experimental apparatus and are
156 the focus of this study. Two specific PFAA will be highlighted, PFHxA and PFHxS, as they have
157 become broadly used in place of PFOA and PFOS and recently have been oft detected in
158 environmental matrices; three additional PFAS compounds, two long chain (>C7) PFCA and one
159 fluorotelomer sulfonate were also included in the study.

160 **Passive Sampler Assembly.** The assembly of the tube passive samplers for PFAS was
161 based on the method outlined by Fauvelle et al, 2017.²³ Microporous polyethylene tubes purchased
162 from the Pall Corporation (Filtroplast, 12 mm O.D., 8 mm I.D. 35% porosity, 2.5 um pore size, 0.6 g
163 cm⁻³ density) were cut into 7 cm long sections. These 7 cm long tube sections were then submerged
164 in a 24-hour EtOH wash which was followed by a 24-hour LC-MeOH wash. Once fully dry, one end
165 of the tube was closed using a snap-in polyethylene cap purchased from McMaster Carr, and 600
166 mg of Oasis hydrophilic lipophilic balance (HLB) sorbent was measured out and poured inside the
167 open end of the tube. HLB sorbent was chosen as opposed to weak anion exchange (WAX) due to
168 its affinity for a wider range of chemistries aside from just anionic PFAS, which will be vital to future
169 applications.²⁰ Prior to deployment in the laboratory, assembled tube samplers were conditioned for
170 at least 24 hours in LC-MeOH, followed by 24-hours in LC-water. The tube samplers were then
171 either immediately deployed into the laboratory, field, or stored in LC-water until the experiment
172 began.

173 **Passive Sampler Extraction.** Immediately following deployment, the tube passive sampler
174 was placed in a 15 mL Falcon Tube and centrifuged at 4000 rpm for 2 minutes using an Eppendorf
175 Centrifuge 5810 (Fisher Scientific, USA) to remove any water remaining in the tube membrane or
176 sorbent. This centrifugation step is repeated until no further water is collected in the bottom of the
177 tube. At this point, the tube was either frozen for future extraction after a maximum of six months or

178 extracted immediately using liquid solid extraction (LSE). Tube samplers were submerged in
179 approximately 6 mL of LC-grade MeOH that had been spiked with a mass labeled surrogate
180 standard (MPFAC-30ES+3) within a 15 mL Falcon tube. After 24 hours, this methanol extract was
181 collected in a pre-labeled, pre-cleaned Falcon tube. The tube sampler was centrifuged as previously
182 described to remove any additional LC-MeOH, which was added to the collected extract. The
183 sampler was then extracted in another 6 mL of LC-grade MeOH, resulting in roughly 12 mL total of
184 extract. The extract was concentrated to approximately 0.5 mL in total volume under a gentle stream
185 of Nitrogen while heated to 35°C. An aliquot of this final concentrate was diluted with 4 mM
186 Ammonium Acetate in water and prepared for analysis via liquid chromatography tandem mass
187 spectrometry (LC/MS/MS)

188 **Instrumental Analysis.** LC/MS/MS analysis was performed at the University of Rhode
189 Island on a Shimadzu Prominence liquid chromatograph (UFLC) coupled to SCIEX TripleQuad 5500
190 MS/MS operating in negative mode for all laboratory and most field samples. Field samples
191 collected in on Cape Cod were analyzed at Harvard University using an Agilent 6460 Triple
192 Quadrupole Liquid Chromatography-tandem Mass Spectrometer following the method in previous
193 work.³⁷ For additional details on the operating conditions, quality assurance, and interlaboratory
194 comparison data refer to Tables S7-S10 in the SI.

195 **Experimental Tank Deployments and Measurements.** To measure laboratory uptake and
196 sampling rates, triplicate tube passive samplers were deployed at four different flow rates (0, 10, 20,
197 and 60 cm s⁻¹) and two different temperatures (15°C and 25°C). Each trial consisted of a 14-day
198 deployment, where duplicate 50 mL water grab samples were taken at the beginning and end of
199 each deployment to verify PFAS concentrations during deployments (Fig S3). Water samples were
200 extracted and analyzed in accordance with methods detailed in literature and used to calculate
201 sampling rates for corresponding individual passive samplers using equation 4.^{36,39} For additional
202 details on the experimental tank design and construction, see SI.

203 **PFAS Uptake by HDPE Membranes and HLB Sorbent.** As part of the validation process of
204 this passive sampler design and model, partitioning was measured for PFAS between the
205 microporous polyethylene membrane (K_{mw}) and water (K_{sw}). Two complementary approaches were
206 used to quantify K_{mw} values reflecting different deployment conditions: (1) Batch experiments on a
207 shaker table (low flow) were performed in conjunction with (2) deployments of membranes without
208 sorbent in the experimental tank at high water flows. Batch experiments, with either sorbent or tube
209 membranes without sorbent were deployed in bottles of LC-grade water spiked with a known
210 concentration of PFAS compounds. K_{mw} trials were specifically important to understanding the
211 uptake of PFAS into the sampler due to the predicted high resistance to uptake of the membrane
212 phase. For additional details on the K_{sw} methods, see SI.

213 **Uptake by Bio Fouled Tube Membranes.** Field deployments might incur an additional
214 resistance to uptake from biofouling that is not accounted for in most laboratory and model methods.
215 Clean tubes were left in a riverine environment for one month to naturally bio foul. These tubes were
216 then re-conditioned (as above) and deployed in the experimental tank alongside freshly prepared
217 tubes at two similar temperatures and two distinct flow speeds (0 and 60 cm s⁻¹) to investigate
218 potential interferences of biota and environmental detritus on uptake through the microporous
219 membrane.

220 **Field Deployments.** Passive samplers were deployed in the field for 14-28 days at three
221 locations, including AFFF-impacted groundwater (JBCC) and river (QR9) downstream of a former
222 fire training area on Joint Base Cape Cod, MA (USA) and a river downstream of a historical textile
223 mill in Westerly, RI (Pawcatuck). Groundwater deployments (n = 3) were conducted for 14 days in
224 June 2021 in a previously characterized PFAS plume⁴⁰ where the average linear groundwater
225 velocity is 0.0005 cm s⁻¹. River deployments occurred between October 2019 and September 2020
226 at QR09 (n = 9), and in May 2021 at Pawcatuck (n = 2). Grab samples of surface and groundwater
227 were collected during deployment and/or recovery of passive samplers and extracted in the manner

228 described in previous literature by either the University of Rhode Island or Harvard University.^{36,39,41}
229 For additional environmental and field QA/QC details, see SI.

230 **Development of a Numerical Model.** A correlation between aqueous diffusion coefficients
231 for 5 PFCA at 20 °C reported by Schaefer et al. and the number of fluorinated carbons was used to
232 derive best fit D_w values. These diffusivities were then applied to calculate mass transfer coefficients
233 (MTC) through the water boundary layer, microporous membrane layer, and sorbent layer for each
234 compound (eqn 2, eqn 5, Table S3).⁴² We assumed that transport is entirely through the pore space
235 of the microporous membrane and that the only diffusion within the sorbent layer is from aqueous
236 diffusion within the water saturated interior, as in prior work.³² Diffusion coefficients were adjusted to
237 reflect the change in temperature in these experiments (15-25 °C) using equation 6.⁴³

238
$$\frac{D_{T1}}{D_{T2}} = \frac{T_1}{T_2} * \frac{v_{T2}}{v_{T1}} \text{ (eqn 6)}$$

239 Where D is the aqueous diffusivity at two given temperatures ($T1$ and $T2$),

240 And v is the dynamic viscosity of water at a given temperature.

241

242 **Results & Discussion**

243 **Validation of tube passive sampler.** Laboratory experiments were conducted to investigate
244 the impact of temperature, flow rate, deployment length and biofouling on the sampling rates of the
245 target PFAA by the PE-tube passive sampler. Sampling rates were calculated for laboratory and
246 field observed samplers using equation 4. To be able to predict sampling rates, laboratory
247 experiments were completed to independently quantify PFAS sorption to the HDPE membrane and
248 the HLB sorbent of the passive sampler. With those values, the predicted model sampling rates
249 were then compared to the field and laboratory observed sampling rates.

250 **Sampling Rates of PFAS by PE tube samplers in laboratory experiments.** Sampling
251 rates of PFAA by the tube passive sampler in the laboratory experiments increased with chain
252 length. For example, for PFCA, average sampling rates across 10-60 cm s⁻¹ water flow increased

253 from PFBA (12 ± 6), to PFPeA (18 ± 5 mL day⁻¹) to PFHxA (120 ± 51 mL day⁻¹), and PFOA ($120 \pm$
 254 55 mL day⁻¹) at 25°C . PFSA had higher overall sampling rates than PFCA but displayed the same
 255 trend in chain length between PFBS, PFHxS, and PFOS (Table 1). To assess the impact of
 256 environmental variables of these sampling rates, the influence of water velocity and temperature on
 257 sampling rates was investigated.

258 **Table 1. Sampling Rates For 9 PFAA.** Laboratory and field observed sampling rates for 9 PFAA compounds of interest
 259 compared to two different derivations of a model for predicting sampling rates at three temperatures for flow rates between 0.5-60
 260 cm/s. All observed values display one standard deviation, all predicted models display the uncertainty associated with the predicted value in
 261 the same units. Lab observed sampling rates were derived from 14-day deployments while field observed were 21-32 days in
 262 length.

Compound	Temp °C	Lab Observed Rs (mL day ⁻¹) n = 3	Field Observed Rs (mL day ⁻¹) n = 11	Field Observed Rs (Gardiner et al. 2022)	EQN 2 Rs Low K _{mw} (mL day ⁻¹)	EQN 2 High K _{mw} (mL day ⁻¹)	EQN 5 Rs (mL day ⁻¹)
PFBA	5		16 (±06)		3.7 (±1.3)	63 (±33)	14 (3.9)
	15	22 (±12)	11 (±05)	7.3 (±5.5)	5.1 (±1.8)	86 (±45)	19 (5.3)
	25	12 (±6)			6.7 (±2.3)	110 (±59)	25 (7.0)
PFBS	5		44 (±20)		2.9 (±1.0)	89 (±46)	13 (3.6)
	15	40 (±11)	67 (±24)	22(±7.9)	4.1 (±1.4)	120 (±63)	18 (5.0)
	25	100 (±57)			5.3 (±1.9)	160 (±83)	23 (6.4)
PFPeA	5		30 (±11)		2.9 (±1.0)	8.7 (±4.5)	13 (3.6)
	15	18 (± 5)	35 (±18)	12 (±2.9)	4.1 (±1.4)	12 (±6.2)	18 (5.0)
	25	45 (±7)			5.3 (±1.9)	16 (±8.3)	23 (6.4)
PFHxA	5		37 (±13)		3.6 (±1.3)	35 (±18)	11 (3.1)
	15	100 (±81)	46 (±40)	18 (±5.5)	5.0 (±1.8)	48 (±25)	15 (4.2)
	25	120 (±51)			6.6 (±2.3)	63 (±33)	19 (5.3)
PFHxS	5		55 (±28)		26 (±9.2)	89 (±46)	8.7 (2.4)
	15	94 (±31)	67 (±28)	23 (±10)	35 (±13)	120 (±63)	12 (3.4)
	25	200 (±72)			48 (±17)	160 (±83)	16 (4.5)
PFHpA	5		46 (±20)		2.9 (±1.0)	58 (±30)	8.7 (2.4)
	15	72 (±60)	59 (±15)	23(±7.0)	3.9 (±1.4)	79 (±41)	12 (3.4)
	25	200 (±130)			5.2 (±1.8)	100(±54)	16 (4.5)
PFHpS	5		41 (±23)		12 (4.1)	120 (60)	6.8 (1.9)
	15	100 (±110)	120 (±83)	17 (±2.5)	16 (±5.7)	160 (±82)	9.4 (2.6)
	25	280 (±110)			21 (±7.5)	210 (±110)	12 (3.4)
PFOA	5		41 (±19)		6.2 (±2.2)	37 (±19)	6.8 (1.9)
	15	62 (±16)	58 (±10)	23 (±5.1)	8.5 (±3.0)	52 (±27)	9.4 (2.6)
	25	120 (±55)			11 (±3.9)	68 (±35)	12 (3.4)
PFOS	5		38 (±22)		19 (±6.8)	190 (±100)	4.9 (1.4)

	15	400 (±160)	63 (±24)	23 (±7.5)	27 (±9.4)	260 (±130)	6.7 (1.9)
	25	290(±110)			35 (±12)	340 (±180)	8.8 (2.5)

263

264

265

266

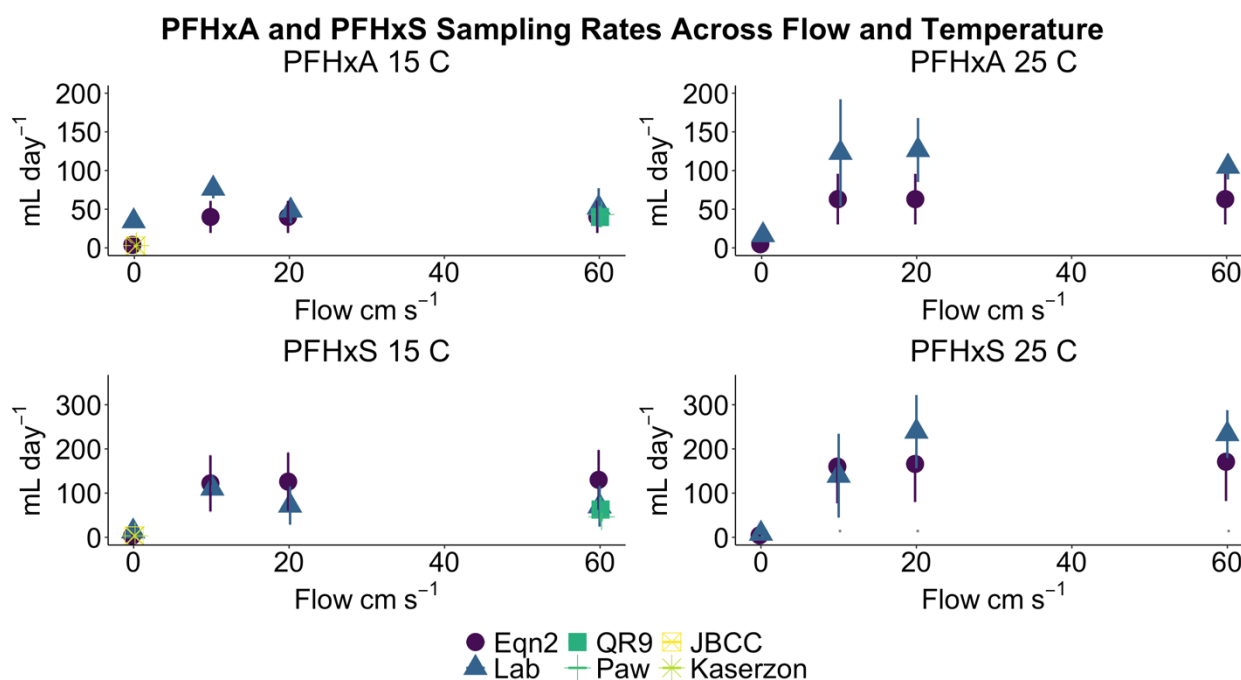
267

268

269

270

Influence of water flow velocity on Rs. For PFHxA and PFHxS, sampling rates were not a function of flow rate between 10-60 cm s⁻¹ for laboratory and field observed, or equation 2 modeled sampling rates (Fig 1). Observed sampling rates did also not change as a function of water flow for the other PFAS (Table 1). The lack of water flow effect on sampling rate extended down to 0.5 cm s⁻¹ based on the model (eqn 2) for flow rates below the 10 cm s⁻¹ limit of most handheld flow meters. A lower value of approximately 0.5 cm s⁻¹ flow speed is predicted to result in similar sampling rates as those seen between 10-60 cm s⁻¹ (Figure S4 and S5).



271

272

273

274

275

276

FIGURE 1. Modeled and observed sampling rates of PFHxA and PFHxS at two temperatures in the field deployments (15 °C) and laboratory experiments (15 and 25 °C). Error bars display 1 standard deviation for measurements and propagated uncertainty for modeling data. Figure includes previous groundwater deployments of this passive sampler by Kaserzon et al.²⁴

277 **Influence of temperature on Rs.** The laboratory observed sampling rates increased for
278 PFAA with increasing (10 °C) temperature. The sampling rate increase with temperature for the tube
279 passive sampler was greater for PFSA, on average by 46%, than for PFCA of similar chain length
280 (Table 1, Fig 1, Fig S5). This increase is reflective of diffusivity's dependency on temperature, which
281 was accounted for in the model development and application to accurately predict a 40% increase in
282 sampling rate differences between 15 and 25 °C. Additionally, the 25 °C laboratory observations
283 exhibited a larger standard deviation in sampling rate amongst replicates than what as observed in
284 the 15 °C or field observed sampling rates.

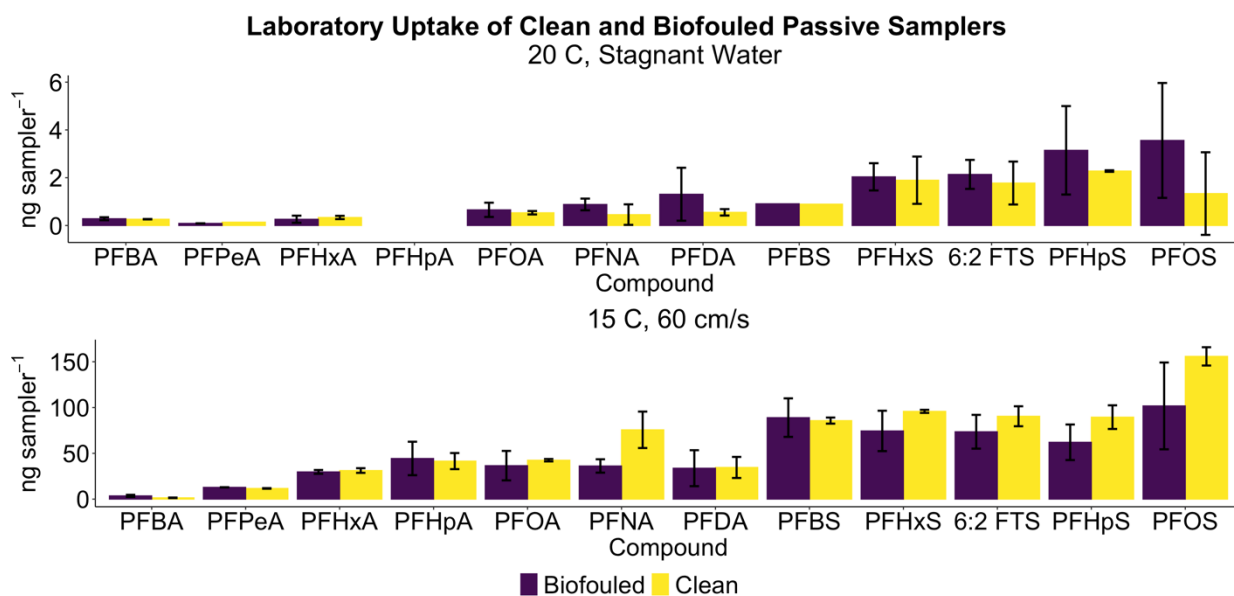
285 **Uptake of PFAS by Biofouled tubes.** To validate the performance of these passive
286 samplers under field conditions, biofouling might introduce an additional resistance to uptake. There
287 was no obvious difference between the mass of PFAS on clean and bio fouled tubes during
288 concurrent laboratory experiments (Fig 2). This could be explained by considering how a thin, high
289 water-content layer of algae, sponge, or other organic matter (Figure S8) compares to the thick
290 polyethylene membrane in thickness and permeability^{45,46}. However, biofouling conditions are very
291 difficult to recreate in the laboratory, and the conditioning of these field-exposed tubes likely altered
292 the biofouling layer. Further experiments, such as tube deployments in a laboratory setting with live
293 algae/bacteria might be necessary to better assess the impact of biofouling on PFAS uptake.

294 To further explore this question, a fourth term was added to equation 2 to account for the
295 uptake resistance introduced by a bio fouled membrane. We estimated the thickness of the
296 biological layer to be 0.04 cm based on observation, and used reported K_{oc} values as a proxy for the
297 affinity of PFAS to the organic material in the bio fouled layer:⁴⁷

298
$$\frac{1}{k_o} = \frac{1}{k_w} + \frac{d_m}{K_{mw}*(D_w*\phi_m)} + \frac{d_s}{K_{sw}*(D_w*\phi_s)} + \frac{d_b}{K_{oc}*(D_w*\phi_b)} \text{ (eqn 7)}$$

299
300 The addition of the biofouled layer as parameterized above resulted in a 0.2-2% decrease in
301 the modeled sampling rate for PFHxA and PFHxS at 15 and 25 °C, which is insignificant when

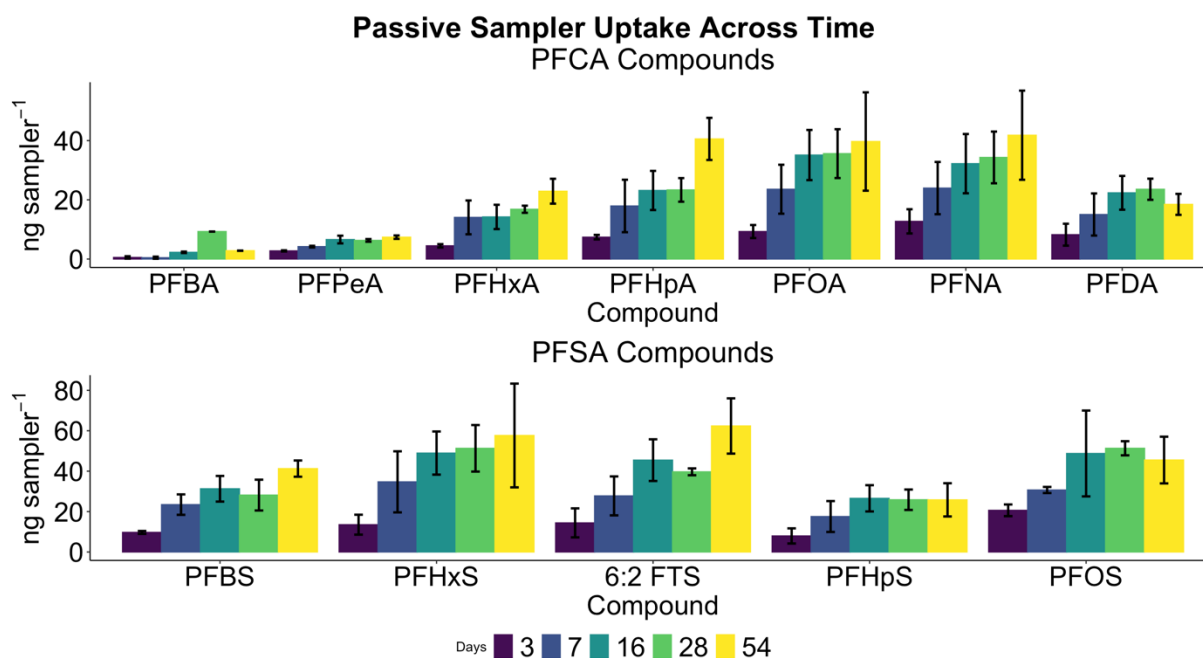
302 compared to the 52% uncertainty within the model. These considerations indicated the kinetic
 303 impact on sampling rate can be neglected when predicting sampling rate of a field deployed passive
 304 sampler, though physical issues such as pore blockage or sorbent congestion may remain a
 305 concern. Using the equation 7, a 1 cm thick layer of biofouling was calculated to be the limit at which
 306 the sampling rate would decrease by more than 25% for PFHxA and PFHxS at flow speeds >0.5 cm
 307 s⁻¹.



308
 309 **FIGURE 2. Comparison of mean PFAS mass (ng) measured in co-deployed tube samplers**
 310 **under similar conditions in the experimental tank.** Error bars are 1 standard deviation of the
 311 mean.

312
 313 **Uptake of PFAS Over Time.** Replicate passive samplers were deployed for 3, 7, 16, 28, and
 314 54 days in the experimental tank to determine the length of time in which there is a net uptake of
 315 PFAS. The results suggest that linear uptake was maintained for most compounds between 0-16
 316 days (Fig 3). As molecular weight increased, curvi-linear uptake and potential saturation at the
 317 sorbent/membrane interference by high molecular weight compounds was exhibited between 16 and
 318 54 days (Fig 3). For example, uptake of PFDA, PFHpS, and PFOS seemed to cease, exhibiting no

319 visible increase in mass after 16 days. PFPeA, PFHxA, PFHpA, PFOA, PFNA, PFBS, PFHxS, and
 320 6:2 FTS showed likely curvi-linear uptake as little to no increase in mass was exhibited between 16-
 321 28 days before increases were observed at 54 days. The apparent reduced uptake of PFAS
 322 observed here could be explained by electrostatic repulsion of diffusing compounds within the pore
 323 space of the PE membrane once it PFAS have covered its surface (see below). These results
 324 suggest that a shorter deployment length of 14 days should be used to ensure all compounds
 325 remain in or close to the linear uptake during sampler deployment. For high molecular weight
 326 PFSA's like PFHxS, PFHpS, and PFOS, this could explain the discrepancy between field sampling
 327 rates being lower than both laboratory and model-derived sampling rates.



328
 329 **Figure 3. Mean uptake (ng) of PFAS by replicate passive samplers over 3, 7, 16, 28 and 54**
 330 **days** (Error bars are 1 standard deviation).

331
 332 **Sampling Rates of PFAS in the field.** PFHxA displayed sampling rates of 40 ± 10 mL day⁻¹
 333 in the riverine field deployments at >20 cm s⁻¹ water velocity for 21-32 days at two temperature
 334 profiles, 5 and 15°C (Table 1). These values are not different given the overlapping uncertainties with

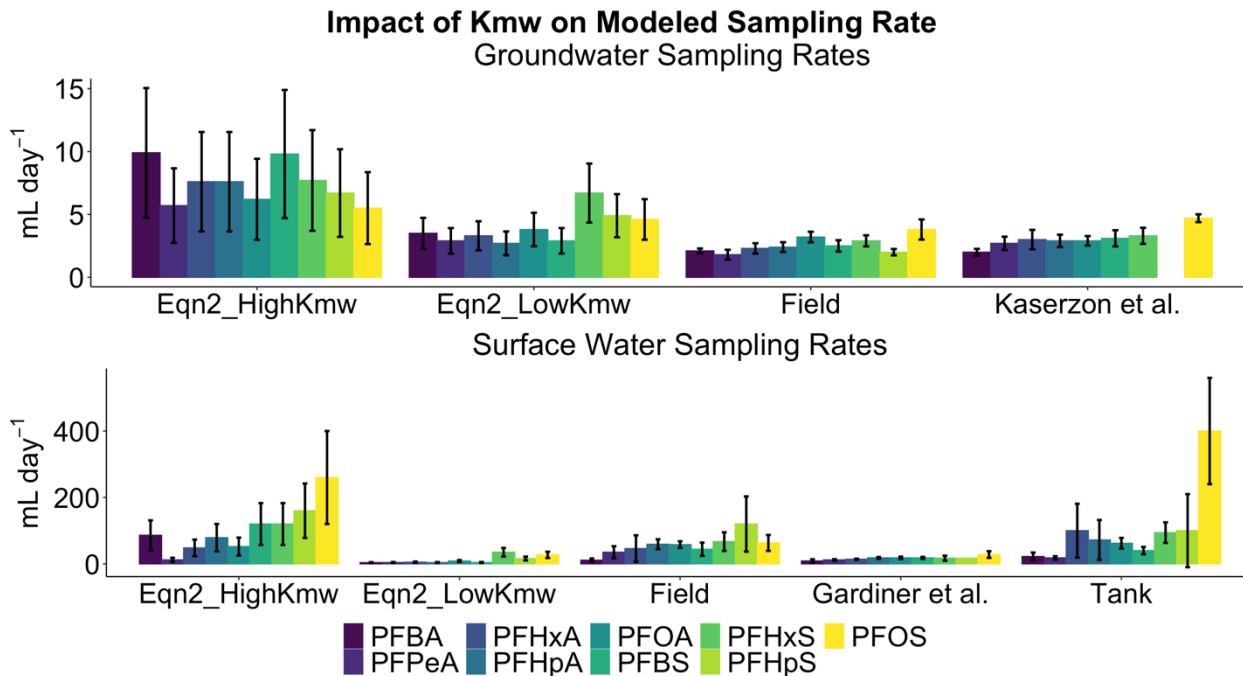
335 the laboratory observed sampling rates (100 ± 81 mL day⁻¹) and model predicted sampling rates (48
336 ± 25 mL day⁻¹). Sampling rates for PFHxS showed slight differences between the field values (50
337 ± 20 mL day⁻¹) and the similar laboratory (120 ± 63 mL day⁻¹) and modeled (110 ± 53 mL day⁻¹)
338 sampling rates. Field sampling rates could be lower than model or laboratory derived sampling rates
339 due to their longer (14 versus 28-32 day) deployment lengths. Tube passive samplers deployed in
340 the field displayed lower variance than laboratory observed passive samplers with an average
341 standard deviation of 43% in the field replicates compared to 61% in the laboratory. The high
342 variance in the lab measured sampling rates likely reflects the high standard deviation in the lab
343 measured K_{mw} values from the tank experiments (Table S6).

344 Passive samplers deployed in the field in this experiment exhibited higher sampling rates
345 than those reported by a recent study using this design in waste water treatment plant effluent
346 (Table 1).⁴⁴ PFHxA field sampling rates in two high flow rivers reported in this study were 46 ± 40 mL
347 day⁻¹ compared to 18 ± 5.5 mL day⁻¹ from literature. One explanation could be the low flow, heavily
348 polluted nature of the waste water treatment plant environment suppressing uptake of PFAS (i.e.
349 PFAS were effectively outcompeted) compared to surface waters and experimental lab settings
350 discussed in this study.

351 Passive samplers deployed in ground water conditions exhibited comparable sampling rates
352 to a previous study using the same tube passive sampler design for PFAS monitoring in
353 groundwater.²⁴ In this study, sampling rates measured ranged from 1.8 – 3.2 mL day⁻¹ for PFBA,
354 PFPeA, PFHxA, PFHpA, and PFOA compared to 2.0-3.0 mL day⁻¹ for the same compounds
355 reported by Kaserzon et al. 2019.²⁴

356 **Uptake of PFAS by PE Tube.** For the parametrization of the uptake model using equation 2,
357 the K_{mw} values are of great importance. Surprisingly, we observed results a difference of almost an
358 order of magnitude between the low flow batch experiment and tank experiment derived K_{mw} values
359 (e.g., for PFOA 0.55 g Water/g HDPE vs 3.5 g Water/g HDPE) (Table S6). In both sets of data the
360 uptake of PFAA by the empty PE tube membranes increased with chain length. PFSA exhibited

361 higher partitioning values between membrane-water phases than their PFCA homologues (Table
362 S6). Published values for PFAA partitioning to PE were limited, though a published value for PFOS
363 partitioning to PE was within 20% of the high flow K_{mw} value for PFOS reported in this study.⁴⁸
364 Diffusion through membrane was calculated to be the largest resistance to uptake between the three
365 phases of this passive sampler design (Fig S7) thus validating the use of this sampling rate model
366 instead of a diffusion model for predicting uptake.³⁷ We hypothesize that the presence of flow
367 disrupts the water boundary layer significantly, allowing more PFAS compounds to diffuse and
368 adsorb into the interior pore spaces of the membrane. This increase in K_{mw} is significant to the
369 accuracy of the model, as Figure 4 displays that how the predictions of sampling rate from low K_{mw}
370 values better align with our measured groundwater sampling rates as well as previously published
371 samples.²⁴ Similarly, the higher K_{mw} derived estimates better represent the field and laboratory tank
372 measured sampling rates of this study (Fig 4). However, these higher values from the tank
373 experiments show greater variability and K_{mw} values must be better constrained to improve this
374 model approach going forward. For this reason, we suggest using the tank derived K_{mw} values for
375 surface waters with flow of $>0.5 \text{ cm s}^{-1}$ and using the batch experiment K_{mw} values for ground water
376 sampling rate predictions.



377

378 **FIGURE 4. Influence of low and high K_{mw} values on equation 2 modeling approach in**

379 **groundwater and surface water.** Error bars display either standard deviation of field/laboratory

380 replicates or uncertainty of the model. Data is included from previous field deployments of this

381 passive sampler design by Kaserzon et al. 2019 in groundwater and Gardiner et al. 2022 in waste

382 water treatment effluent.^{24,44}

383

384 **Uptake of PFAS by sorbent.** Uptake of PFAS by the HLB sorbent generally increased with

385 chain length (Table S6) for PFCA and PFSA. Log K_{sw} ranged from 2.7 for C4 (PFBA) to 6.0 for C9

386 (PFNA) and were in good agreement with previous literature (3.5-5.7).²⁵ PFSA displayed greater log

387 K_{sw} values than PFCA: 4.8 for PFBS, and a linear increase from PFHxS to PFOS (Log K_{sw} 4.2-5.6)

388 which were also in line with reported values (4.2-5.3 for PFBS, PFHxS, and PFOS)(Table S6).³⁴

389 Sorption to HLB was consistent, with an average standard deviation of 3.4%, suggesting that the

390 uptake of PFAS by the HLB sorbent is not a major source of uncertainty in the model derived

391 sampling rate predictions. K_{sw} values were consistently much greater than K_{mw} values, indicating that

392 the HLB sorbent is the main receiving phase for any PFAS taken up by the passive sampler. For

393 future applications, an understanding on how environmental matrices will impact K_{sw} values should
394 be investigated as well.

395 **Comparison to other Passive Samplers for PFAA.** The observed PFAS sampling rates
396 were compared to published sampling rates from other integrative passive samplers, normalized to
397 sampler surface area.^{20,32,33} The tube passive sampler displayed a surface-normalized sampling rate
398 ($R_s/Area$, or mass transfer) of almost an order of magnitude higher than the standard POCIS design
399 (Table S5). The mass transfer fell within the ranges reported for DGT samplers, though it was lower
400 than the reported modified POCIS method developed with a smaller surface area (Table S5)

401 **Comparison of two Modeling Approaches for Sampling Rate.** The core difference
402 between these two approaches is that equation 2 includes partitioning to the membrane and
403 sorbent, in addition to diffusion, while equation 5 models uptake rates based on diffusion only.

404 Several lines of evidence imply that sorption to the membrane is important. Both this study
405 and two other studies using this tube sampler design for PFAS display a general increase in
406 sampling rate with chain length (Table 1).^{24,44} Equation 2 is impacted by the K_{mw} values used,
407 serving as a modifier that shows an increase in sampling rate with chain length and molecular mass
408 (PFPeA 12 mL day⁻¹ to PFOA 52 mL day⁻¹ at 15 °C). An increase in sampling rate from equation 2
409 compared to the equation 5 model (Fig 4, Table S6) is observed for compounds that exhibit K_{mw}
410 values greater than 1. In contrast, when K_{mw} is less than 1 in the low flow regime, we see a decrease
411 in equation 2 sampling rates relative to equation 5 (Fig 4, Table 1). Taking PFHxS for example,
412 equation 2 predicts a 120 (± 63) mL day⁻¹ versus 12 (± 3.4) mL day⁻¹ from equation 5. Equation 5
413 also shows a decrease in sampling rate with chain length, as partitioning considerations are
414 simplified out of the math, a trend contrary to this study's data and previous publications^{24, 44}. Both
415 models do exhibit flow resistance between 0.5-60 cm s⁻¹ in modeled sampling rate predictions,
416 indicating that the thickness of the membrane still plays a vital role in both estimates (Fig S4, S5).
417 The propagated error of both models was 52% equation 2 with equation 5 at 29% based off
418 uncertainties in the terms of each model such as K_{mw} , K_{sw} , and diffusivity. These results suggest that

419 equation 5 may be the most appropriate approach for explaining sampling rates, with further
420 refinement necessary.

421 **Comparison of Model, Laboratory, and Field Sampling Rates.** Ultimately, equation 2
422 seem best suited for predicting uptake rates when compared to the field and laboratory data: PFHxA
423 exhibited sampling rates ranged from 37-46 mL day⁻¹ at two temperatures in the field, while equation
424 2 models predicted 35-48 mL day⁻¹ (while equation 5 predicted 11-15 mL day⁻¹).

425 For shorter chain compounds with lower anticipated partitioning to the membrane, equation 5
426 overestimates sampling rate when compared equation 2 (Table 1). PFBA had field and laboratory
427 Rs values of 11 (± 5.0) and 22 (± 12) mL day⁻¹ respectively at 15 °C, compared to the predictions of
428 86 ± 45 (eqn 5) and 5.1 ± 1.8 mL day⁻¹ (eqn 2). This is likely due to overestimated K_{mw} for these
429 shorter, more polar compounds and requires further study. PFHxS displayed field values at 15 °C of
430 67 ± 28 , with modeled sampling rates of 120 ± 63 (eqn 2) and 12 ± 3.4 mL day⁻¹ (eqn 5).

431 Laboratory measured samples rates were anomalously high in comparison to field and both
432 model predictions (Table 1, Fig 1). This is likely because of the lack of environmental matrix, which
433 could compete with PFAS for binding sites on the membrane surface and within the HLB sorbent. In
434 addition, the significant difference we observed in K_{mw} values from either batch or tank experiments
435 seems to suggest that sorption to the membrane can be enhanced in higher-flow environments.
436 PFHxA sampling rates in the laboratory were almost double that of the sampling rates in the field
437 (100 ± 81 vs 46 ± 40 mL day⁻¹).

438 **Environmental Implications.** In this study, the tube passive sampler was shown to take up
439 PFAA with 4-8 carbon chain lengths in a predictable manner in the field. The resistance to varying
440 water flows exhibited by the tube passive sampler in both the laboratory and model estimations for
441 sampling rates (Fig 1, S4, S5) provided an advantage for widespread deployments in surface waters
442 without the need for site specific calibration. These Rs models can easily be tweaked for
443 temperatures outside of the 15-25 °C discussed here, and a predicted sampling rate, or range of

444 sampling rates, can be applied to riverine or estuarine flows $>0.5 \text{ cm s}^{-1}$. Further investigation of low
445 flow conditions may be necessary for broad groundwater deployments, though the initial measured
446 sampling rates in groundwater from this study were in good agreement with previously reported
447 data.²⁴ Overall, the sampler promises to be a simple tool that can be used to screen for PFAS
448 concentrations in environmental waters.

449 Future work could investigate a sorbent other than HLB might increase sampler uptake over
450 time and reduced the potential matrix effect in environmental waters. Sampling rates for the tube
451 membrane (without sorbent) were lower than all model, field, or laboratory-measured sampling rates
452 for the tube passive sampler, indicating that the membrane is not the major reservoir for PFAS in the
453 sampler (Fig S6). This suggests that the leveling off of uptake exhibited between 16-54 days could
454 be due to sorbent congestion or inefficient transport of PFAS through the membrane layer. The
455 determination of accurate aqueous diffusion coefficients and K_{mw} values for many PFAS compounds
456 is essential to improving the accuracy and application of this work.

457 Based on the field and laboratory results presented here, we suggest the use of the equation
458 2's predicted sampling rates for 14-day deployments, while additional work is needed to better
459 constrain the importance of K_{sw} and K_{mw} values within the model estimates. It is clear from this work
460 that K_{mw} is an important term to include in the model to reflect an increase in sampling rate with
461 chain length, making equation 5 a poor choice. However, equation 2 shows high sensitivity to the
462 K_{mw} values, with sampling rates suppressed by K_{mw} lower than 1 in ground water deployments.
463 Future directions should characterize the change in these partitioning values in the presence of
464 environmental matrix, while expanding the number of compounds and methods for PFAS detection
465 that this sampler design is validated for detecting in surface and ground waters.

466

467

468 Associated Content

469

470 **Supporting Information**

471 The Supporting Information is available free of charge on the ACS Publications website at DOI:

472 It contains additional analytical details, methods, standards, quality control and assurance, LC/MS
473 conditions, details on field deployment sites and conditions, sampling rates for 9 PFAA compounds
474 of interest, images of experimental tank setup and bio fouled passive samplers recovered from the
475 field, interlaboratory comparison data and results.

476

477 Author Information

478 Corresponding Author

479 Email: rlohmann@uri.edu. Phone (401)874-6612

480 ORCID

481 Matthew Dunn: 0000-0002-8902-8434

482 Jitka Becanova: 0000-0002-3091-1054

483 Jarod Snook:

484 Bridger Ruyle: 0000-0003-1941-4732

485 Rainer Lohmann: [0000-0001-8796-3229](https://orcid.org/0000-0001-8796-3229)

486

487

488 **Notes**

489 The authors declare no competing financial interest.

490

491 **Acknowledgements**

492 The authors acknowledge funding from the Department of Defense's Strategic and Environmental
493 Research Development Program (Grant # ER18-1280) and the URI STEEP Superfund Research
494 Center (P42ES027706). We thank Denis LeBlanc (USGS), Nicholas Noons and Kirsten Bailey
495 (Rhode Island Department of Environmental Management), Thomas Garrows, Melissa Woodward,

496 Asta Habtemichael, Anna Robuck, and Izak Hill (all URI) for field support, and Dr. Kees Booij
497 (PaSOC) for valuable comments on a previous version of this manuscript.

498

499

500 **References**

- 501 1. Buck, R. C., Franklin, J., Berger, U., Conder, J. M., Cousins, I. T., Voogt, P. de, Jensen, A.
502 A., Kannan, K., Mabury, S. A., & van Leeuwen, S. P. J. (2011). Perfluoroalkyl and
503 polyfluoroalkyl substances in the environment: Terminology, classification, and origins.
504 *Integrated Environmental Assessment and Management*, 7(4), 513–541.
505 <https://doi.org/10.1002/ieam.258>
- 506 2. Schaider, L. A., Balan, S. A., Blum, A., Andrews, D. Q., Strynar, M. J., Dickinson, M. E.,
507 Lunderberg, D. M., Lang, J. R., & Peaslee, G. F. (2017). Fluorinated compounds in U.S. fast
508 food packaging. *Environmental Science and Technology Letters*, 4(3), 105–111.
509 <https://doi.org/10.1021/acs.estlett.6b00435>
- 510 3. Houtz, E. F., Higgins, C. P., Field, J. A., & Sedlak, D. L. (2013). Persistence of perfluoroalkyl
511 acid precursors in AFFF-impacted groundwater and soil. *Environmental Science &*
512 *Technology*, 47, 8187-8195 <https://doi.org/10.1021/es4018877>
- 513 4. Wang, Z., Dewitt, J. C., Higgins, C. P., & Cousins, I. T. (2017). A Never-Ending Story of Per-
514 and Polyfluoroalkyl Substances (PFASs)? *Environmental Science and Technology*, 51,
515 2508–2518. <https://doi.org/10.1021/acs.est.6b04806>
- 516 5. Ojo, A. F., Peng, C., & Ng, J. C. (2021). Assessing the human health risks of per- and
517 polyfluoroalkyl substances: A need for greater focus on their interactions as mixtures. *Journal*
518 *of Hazardous Materials*, 407, 124863. <https://doi.org/10.1016/j.jhazmat.2020.124863>
- 519 6. Sunderland, E. M., Hu, X. C., Dassuncao, C., Tokranov, A. K., Wagner, C. C., & Allen, J. G.
520 (2019). A review of the pathways of human exposure to poly- and perfluoroalkyl substances

- 521 (PFASs) and present understanding of health effects. *Journal of Exposure Science and*
522 *Environmental Epidemiology*, 29(2), 131–147. <https://doi.org/10.1038/s41370-018-0094-1>
- 523 7. Cordner, A., de La Rosa, V. Y., Schaider, L. A., Rudel, R. A., Richter, L., & Brown, P. (2019).
524 Guideline levels for PFOA and PFOS in drinking water: the role of scientific uncertainty, risk
525 assessment decisions, and social factors. *Journal of Exposure Science & Environmental*
526 *Epidemiology*, 29, 157-171. <https://doi.org/10.1038/s41370-018-0099-9>
- 527 8. Robuck, A. R., McCord, J. P., Strynar, M. J., Cantwell, M. G., Wiley, D. N., & Lohmann, R.
528 (2021). Tissue-specific distribution of legacy and novel per- and polyfluoroalkyl substances in
529 juvenile seabirds. *Environmental Science and Technology Letters*, 8(6), 457–462.
530 <https://doi.org/10.1021/acs.estlett.1c00222>
- 531 9. Dassuncao, C., Hu, X. C., Zhang, X., Bossi, R., Dam, M., Mikkelsen, B., & Sunderland, E. M.
532 (2017). Temporal shifts in poly- and perfluoroalkyl substances (PFASs) in north atlantic pilot
533 whales indicate large contribution of atmospheric precursors. *Environmental Science and*
534 *Technology*, 51, 4512–4521. <https://doi.org/10.1021/acs.est.7b00293>
- 535 10. Mussabek, D., Ahrens, L., Persson, K. M., & Berndtsson, R. (2019). Temporal trends and
536 sediment–water partitioning of per- and polyfluoroalkyl substances (PFAS) in lake sediment.
537 *Chemosphere*, 227, 624–629. <https://doi.org/10.1016/j.chemosphere.2019.04.074>
- 538 11. Morales-McDevitt, M. E., Becanova, J., Blum, A., Bruton, T. A., Vojta, S., Woodward, M., &
539 Lohmann, R. (2021). The Air That We Breathe: Neutral and Volatile PFAS in Indoor Air.
540 *Environmental Science & Technology Letters*, 8, 897-902.
541 <https://doi.org/10.1021/acs.estlett.1c00481>
- 542 12. Kannan, K., Corsolini, S., Falandysz, J., Fillmann, G., Kumar, K. S., Loganathan, B. G.,
543 Mohd, M. A., Olivero, J., van Wouwe, N., Yang, J. H., & Aldous, K. M. (2004).
544 Perfluorooctanesulfonate and related fluorochemicals in human blood from several countries.
545 *Environmental Science and Technology*, 38, 4489–4495. <https://doi.org/10.1021/es0493446>

- 546 13. OECD.org (2021). Portal on Per and Poly Fluorinated Chemicals. *Organization for Economic*
547 *Co-operation and Development*. [https://www.oecd.org/chemicalsafety/portal-perfluorinated-](https://www.oecd.org/chemicalsafety/portal-perfluorinated-chemicals/countryinformation/european-union.htm#)
548 [chemicals/countryinformation/european-union.htm#](https://www.oecd.org/chemicalsafety/portal-perfluorinated-chemicals/countryinformation/european-union.htm#)
- 549 14. Strong, J. (2016). Lifetime health advisories and health effects support documents for
550 perfluorooctanoic acid and perfluorooctane sulfonate. *Environmental Protection Agency*
551 *Federal Register 81(101)*. [https://www.govinfo.gov/content/pkg/FR-2016-05-25/pdf/2016-](https://www.govinfo.gov/content/pkg/FR-2016-05-25/pdf/2016-12361.pdf)
552 [12361.pdf](https://www.govinfo.gov/content/pkg/FR-2016-05-25/pdf/2016-12361.pdf)
- 553 15. Cousins, I. T., DeWitt, J. C., Glüge, J., Goldenman, G., Herzke, D., Lohmann, R., Miller, M.,
554 Ng, C. A., Scheringer, M., Vierke, L., & Wang, Z. (2020). Strategies for grouping per- and
555 polyfluoroalkyl substances (PFAS) to protect human and environmental health.
556 *Environmental Science: Processes & Impacts*, 22(7), 1444–1460.
557 <https://doi.org/10.1039/d0em00147c>
- 558 16. Lohmann, R. (2012). Critical review of low-density polyethylene’s partitioning and diffusion
559 coefficients for trace organic contaminants and implications for its use as a passive sampler.
560 *Environmental Science and Technology*, 46(2), 606–618. <https://doi.org/10.1021/es202702y>
- 561 17. Booij K, Vrana B, & Huckins J.N. (2007). Theory, modelling, and calibration of passive
562 samplers used in water monitoring. In Greenwood R, Mills GA, Vrana B, eds, *Passive*
563 *Sampling Techniques in Environmental Monitoring*. Elsevier, Amsterdam, The Netherlands,
564 pp 141–169
- 565 18. Harman, C., Allan, I. J., & B auerlein, P. S. (2011). The challenge of exposure correction for
566 polar passive samplers the PRC and the POCIS. *Environmental Science and Technology*,
567 45(21), 9120–9121. <https://doi.org/10.1021/es2033789>
- 568 19. Fauvelle, V., Kaserzon, S. L., Montero, N., Lissalde, S., Allan, I. J., Mills, G., Mazzella, N.,
569 Mueller, J. F., & Booij, K. (2017). Dealing with flow effects on the uptake of polar compounds
570 by passive samplers. *Environmental Science and Technology*, 51(5), 2536–2537.
571 <https://doi.org/10.1021/acs.est.7b00558>

- 572 20. Kaserzon, S. L., Kennedy, K., Hawker, D. W., Thompson, J., Carter, S., Roach, A. C., Booij,
573 K., & Mueller, J. F. (2012). Development and Calibration of a Passive Sampler for
574 Perfluorinated Alkyl Carboxylates and Sulfonates in Water. *Environmental Science &*
575 *Technology*, 46(9), 4985–4993. <https://doi.org/10.1021/es300593a>
- 576 21. Kaserzon, S.L., Vermeirssen, E.L.M., Hawker, D.W., Kennedy, K., Bentley, C., Thompson,
577 J., Booij, K., & Mueller, J.F. (2013). Passive sampling of perfluorinated chemicals in water:
578 Flow rate effects on chemical uptake. *Environmental Pollution*, 177, 58-63.
579 <https://doi.org/10.1016/j.envpol.2013.02.002>
- 580 22. Lai, Y.F., Rauert, C., Gobelius, L., & Ahrens, L. (2019) A critical review on passive sampling
581 in air and water for per- and polyfluoroalkyl substances (PFASs). *Trends in Analytical*
582 *Chemistry*, 121, 115-311. <https://doi.org/10.1016/j.trac.2018.11.009>
- 583 23. Fauvelle, V., Montero, N., Mueller, J. F., Banks, A., Mazzella, N., & Kaserzon, S. L. (2017).
584 Glyphosate and AMPA passive sampling in freshwater using a microporous polyethylene
585 diffusion sampler. *Chemosphere*, 188, 241–248.
586 <https://doi.org/10.1016/j.chemosphere.2017.08.013>
- 587 24. Kaserzon, S. L., Vijayasathay, S., Bräunig, J., Mueller, L., Hawker, D. W., Thomas, K. v., &
588 Mueller, J. F. (2019). Calibration and validation of a novel passive sampling device for the
589 time integrative monitoring of per- and polyfluoroalkyl substances (PFASs) and precursors in
590 contaminated groundwater. *Journal of Hazardous Materials*, 366(September 2018), 423–
591 431. <https://doi.org/10.1016/j.jhazmat.2018.12.010>
- 592 25. Booij, K., Chen, S., & Trask, J. R. (2020). POCIS calibration for organic compound sampling
593 in small headwater streams. *Environmental Toxicology and Chemistry*, 39(7), 1334–1342.
594 <https://doi.org/10.1002/etc.4731>
- 595 26. Endo, S., & Matsuura, Y. (2019). Mechanistic Model Describing the Uptake of Chemicals by
596 Aquatic Integrative Samplers: Comparison to Data and Implications for Improved Sampler Co

597 figurations". *Environmental Science & Technology*, 53, 1482-1489.

598 <https://doi.org/10.1021/acs.est.8b06225>

599 27. Vrana, B., Mills, G., Greenwood, R., Knutsson, J., Svensson, K., & Morrison, G. (2005).

600 Performance optimization of a passive sampler for monitoring hydrophobic organic pollutants
601 in water. *Journal of Environmental Monitoring*, 7(6), 612–620.

602 <https://doi.org/10.1039/b419070j>

603 28. Huckins, J.N., Petty, J., Orazio, C. E., Lebo, J., Clark, R.C., Gibson, V.L., Gala, W.R., &

604 Echols, K.R. (1999). Determination of uptake kinetics (sampling rates) by lipid-containing
605 semipermeable membrane devices (SPMDs) for polycyclic aromatic hydrocarbons (PAHs) in
606 water. *Environmental Science & Technology*, 33, 3918-3923.

607 <https://doi.org/10.1021/es990440u>

608 29. Vrana, B., Mills, G. A., Kotterman, M., Leonards, P., Booij, K., & Greenwood, R. (2007).

609 Modelling and field application of the chemcatcher passive sampler calibration data for the
610 monitoring of hydrophobic organic pollutants in water. *Environmental Pollution*, 145(3), 895–

611 904. <https://doi.org/10.1016/j.envpol.2006.04.030>

612 30. Stephens, B. S., Kapernick, A., Eaglesham, G., & Mueller, J. (2005). Aquatic passive

613 sampling of herbicides on naked particle loaded membranes: Accelerated measurement and
614 empirical estimation of kinetic parameters. *Environmental Science and Technology*, 39(22),

615 8891–8897. <https://doi.org/10.1021/es050463a>

616 31. Booij, K., & Chen, S. (2018). Review of atrazine sampling by polar organic chemical

617 integrative samplers and chemcatcher. *Environmental Toxicology*, 37(7), 1786–1798.

618 <https://doi.org/10.1002/etc.4160>

619 32. Fang, Z., Li, Y., Li, Y., Yang, D., Zhang, H., Jones, K. C., Gu, C., & Luo, J. (2021).

620 Development and applications of novel DGT passive samplers for measuring 12 per- and
621 polyfluoroalkyl substances in natural waters and wastewaters. *Environmental Science and*

622 *Technology*, 55, 9548-9556. <https://doi.org/10.1021/acs.est.0c08092>

- 623 33. Gobelius, L., Persson, C., Wiberg, K., & Ahrens, L. (2019). Calibration and application of
624 passive sampling for per- and polyfluoroalkyl substances in a drinking water treatment plant.
625 *Journal of Hazardous Materials*, 362, 230–237. <https://doi.org/10.1016/j.jhazmat.2018.09.005>
- 626 34. Urik, J., & Vrana, B. (2019). An improved design of a passive sampler for polar organic
627 compounds based on diffusion in agarose hydrogel. *Environmental Science and Pollution*
628 *Research*, 26, 15273-15284. <https://doi.org/10.1007/s11356-019-04843-6>
- 629 35. Wang, P., Challis, J. K., Luong, K. H., Vera, T. C., & Wong, C. S. (2021). Calibration of
630 organic-diffusive gradients in thin films (o-DGT) passive samplers for perfluorinated alkyl
631 acids in water. *Chemosphere*, 263, 128325.
632 <https://doi.org/10.1016/j.chemosphere.2020.128325>
- 633 36. Becanova, J., Saleeba, Z. S. S. L., Stone, A., Robuck, A. R., Hurt, R. H., & Lohmann, R.
634 (2021). A graphene-based hydrogel monolith with tailored surface chemistry for PFAS
635 passive sampling. *Environmental Science: Nano*, 8(10), 2894–2907.
636 <https://doi.org/10.1039/d1en00517k>
- 637 37. Booij, K. (2021). Passive sampler exchange kinetics in large and small water volumes under
638 mixed rate control by sorbent and water boundary layer. *Environmental Toxicology and*
639 *Chemistry*, 40 (5), 1241-1254. <https://doi.org/10.1002/etc.4989>
- 640 38. Glanzman, V., Booij, K., Reymond, N., Weyermann, C., & Estoppey, N. (2021). Determining
641 the mass transfer coefficient of the water boundary layer at the surface of aquatic integrative
642 passive samplers. *Environmental Science & Technology*, 56, 6391-6398.
643 <https://pubs.acs.org/doi/10.1021/acs.est.1c08088?ref=PDF>
- 644 39. Morales-McDevitt, M. E., Dunn, M., Habib, A., Vojta, S., Becanova, J., & Lohmann, R.
645 (2022). Poly- and Perfluorinated Alkyl Substances in Air and Water from Dhaka, Bangladesh.
646 *Environmental Toxicology and Chemistry*, 0(0), 0–2. <https://doi.org/10.1002/etc.5255>
- 647 40. Weber, A.K., Barber, L.B., LeBlanc, D.R., Sunderland, E.M., & Vecitis, C.D. (2017)
648 Geochemical and hydrologic factors controlling subsurface transport of poly- and

649 perfluoroalkyl substances, Cape Cod, Massachusetts. *Environmental Science & Technology*,
650 *51, 8, 4269-4279*. <https://doi.org/10.1021/acs.est.6b05573>

651 41. Ruyle, B.J., Pickard, H.M., LeBlanc, D.R., Tokranov, A.K., Thackray, C.P., Hu, C., Vecitis,
652 C.D., & Sunderland E.M. (2021). Isolating the AFFF signature in coastal watersheds using
653 oxidizable PFAS precursors and unexplained organofluorine. *Environmental Science &*
654 *Technology*, *55, 6, 3686-3695*. <https://doi.org/10.1021/acs.est.0c07296>

655 42. Schaefer, C. E., Drennan, D. M., Tran, D. N., Garcia, R., Christie, E., Higgins, C. P., & Field,
656 J. A. (2019). Measurement of Aqueous Diffusivities for Perfluoroalkyl Acids. *Journal of*
657 *Environmental Engineering*, *145(11)*, 06019006. [https://doi.org/10.1061/\(asce\)ee.1943-](https://doi.org/10.1061/(asce)ee.1943-7870.0001585)
658 [7870.0001585](https://doi.org/10.1061/(asce)ee.1943-7870.0001585)

659 43. Reeks, Michael W. (2011) Stokes-Einstein Equation. *Thermopedia*.
660 <https://www.thermopedia.com/content/1156/>

661 44. Gardiner, C., Robuck, A., Becanova, J., Cantwell, M., Kaserzon, S., Katz, D., Mueller, J., &
662 Lohmann, R. Field validations of a novel passive sampler for dissolved PFAS in surface
663 waters. *Environmental Toxicology and Chemistry*, *41, 10 2375-2385*.
664 <https://doi.org/10.1002/etc.5431>

665 45. Qiang, L., Cheng, J., Mirzoyan, S., Kerkof, L.J., & Haggblom, M.M. (2021). Characterization
666 of microplastic-associated biofilm development along a freshwater-estuarine gradient.
667 *Environmental Science & Technology*, *55, 16402-*
668 *16412*. <https://doi.org/10.1021/acs.est.1c04108>

669 46. Wang, J., Guo, X., and Xue, J. (2021). Biofilm-developed microplastics as vectors of
670 pollutants in aquatic ecosystems. *Environmental Science & Technology*. *55, 12780-*
671 *12790*. <https://doi.org/10.1021/acs.est.1c04466>

672 47. Campos Pereira, H., Ullberg, M., Kleja, D. B., Gustafsson, J. P., & Ahrens, L. (2018).
673 Sorption of Perfluoroalkyl substances (PFASs) to an organic soil horizon – Effect of cation

674 composition and pH. *Chemosphere*, 207, 183–191.

675 <https://doi.org/10.1016/j.chemosphere.2018.05.012>

676 48. Wang, F., Shih, K. M., & Li, X.Y. (2015). The partitioning behavior of

677 perfluorooctanesulfonate (PFOS) and perfluorooctanesulfonamide (FOSA) on

678 micropoplastics. *Chemosphere*, 119, 841-847.

679 <https://doi.org/10.1016/j.chemosphere.2014.08.047>

680

681

682